THE JOURNAL OF PHYSICAL CHEMISTRY B

ARTICLE

pubs.acs.org/JPCB

Modeling Solvatochromism of a Quinolinium Betaine Dye in Water Solvent Using Sequential Hybrid QM/MM and Semicontinuum Approach

N. Arul Murugan*

Department of Theoretical Chemistry, School of Biotechnology, Royal Institute of Technology, SE-10691 Stockholm, Sweden

Supporting Information

ABSTRACT: We have investigated the ambient temperature structure of 1-methyl-8-oxyquinolinium betaine (MOQB) in water solvent and compared to its gas-phase structure. We have employed Car−Parrinello molecular dynamics (CPMD) simulations within hybrid quantum mechanics−molecular mechanics (QM/MM) framework to study MOQB in water while CPMD technique has been used for the gas phase. We report significant solvent-induced geometrical changes in MOQB. The dipole moment of MOQB in water is 2 times larger than the gas-phase value. The average absorption spectra calculated from gas-phase configurations using Coulomb attenuated-B3LYP (CAMB3LYP) level of theory is comparable with experimental spectra reported in benzene (λ_{max} = 590 nm), a nonpolar solvent. We have also computed the absorption spectra of MOQB in water solvent using continuum and semicontinuum solvent models. Based on this, we have calculated contributions from solvent-induced geometrical changes, hydrogen bonding, and intermolecular charge transfer to the solvatochromic shift and absorption spectra of MOQB in water. Absorption spectra calculations for MOQB in water with a semicontinuum approach for solvents using CAMB3LYP level of theory excellently reproduce the experimental spectra in water, where the theoretical λ_{max} is 433 nm and the experimental λ_{max} is around 440 nm.

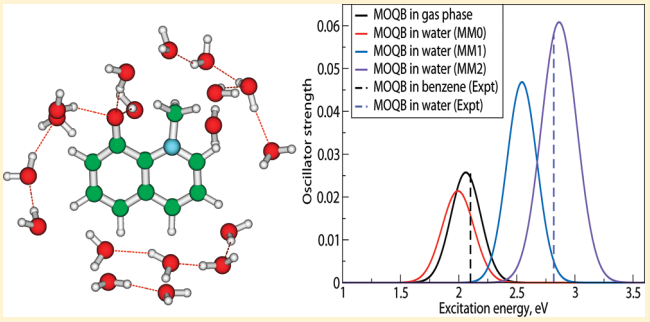

1. INTRODUCTION

The characterization of the dielectric nature of microenvironment of proteins in its folded, unfolded, and misfolded states is essential for drug-design applications and among the molecular probes, fluorosolvatochromic molecules are the immediate candidates for such characterizations. The absorption and fluorescence maximum of the probe molecules are strongly dependent on the micropolarity of the environment[1,2] while the polarity of the protein itself is dependent on its conformational state, and this has been used for various protein characterizations. In addition to protein characterization applications, the fluorosolvatochromic molecules are useful to monitor the microenvironment in the binding sites of proteins,[2] surfactant self-assembly systems,[3] and reverse micelles.[4] Naturally, due to these applications there is growing need to identify small and effective probe molecules. The use of probe molecule becomes less informative and questionable when the probe molecule itself is larger and brings significant geometrical or conformational changes within the systems to be probed. So, it is highly recommended that the probe molecules are significantly small and fit into the microcavity without introducing any changes in the environment for which the polarity has to investigated. In other words, we want that the probe molecules are perturbed by the environment and not vice versa. The second most important requirement is that the probe molecule exhibits considerable solvatochromic shift that is directly proportional to the polarity of the environment and absorbs in the visible region in order to make naked eye detection. Among the very few molecules that meet these requirements, 1-methyl-8-oxyquinolinium betaine (MOQB, see Figure 1) is a molecule belonging to the betaine dye series.[5] The usage of quinolinium betaine molecules has been experimented and found to be successful in the studies of the interfacial solvent and electrostatic characterization of micelles and, unilamellar vesicles, and for both oil-in-water and water-in-oil microemulsions.[6−8] MOQB has been characterized as a negative solvatochromic molecule, and its ground state has been proposed to be in a dipolar charge-separated state.[9] So, in the polar solvents the ground state is stabilized relative to its nonzwitter ionic excited state which leads to increase in the excitation energy, i.e., a blue shift in the absorption maximum.[10] Overall, the relative stabilization of the ground and excited states of MOQB by solvents is dependent on the polarity of the dielectric medium[9−11] which has been exploited for its use in micropolarity characterization.[4,6−8]

The theoretical modeling of structure and absorption spectra of MOQB and other solvatochromic molecules in polar and

Received: May 29, 2010
Revised: December 11, 2010
Published: January 10, 2011

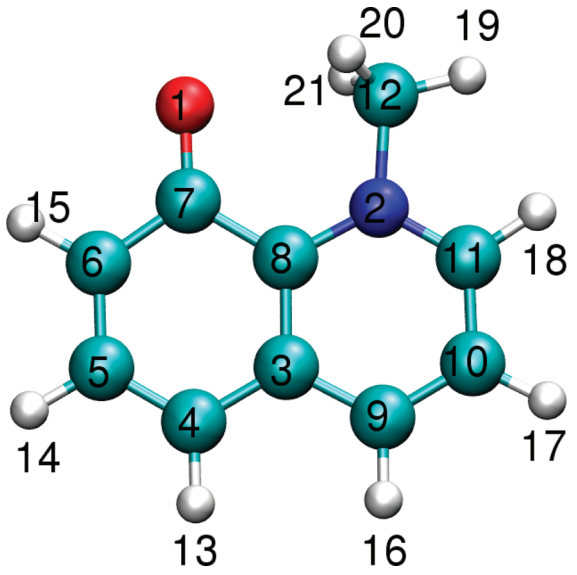

Figure 1. Molecular structure of MOQB.

nonpolar solvents will be useful to establish the structure−property relationships which can be utilized for ab initio design of newer, inexpensive, smaller and efficient probe molecules suitable for a microcavity characterization application. But the modeling of these systems poses difficulties due to considerable solute molecular flexibility, solvent-induced geometrical changes, and the site-specific solute−solvent interaction which demand for a combined use of force-field and ab initio modeling techniques.[12−16] In the solvatochromic systems, the solvent-induced geometrical changes are quite significant.[17−21] It has been reported in the case of phenol blue,[17] merocyanine,[18] and donor-/acceptor-substituted polyenes[19,20] that the change in solvent polarity leads to change in bond-length alternation (BLA) which is defined as the difference between average single and double bond lengths in the conjugation pathway. In addition to change in BLA parameter, there can be conformational change as in *o*-betaine where there is almost 30° change in the twist angle between the two aromatic moieties when the environment changes from gas phase to water solvent.[21,22] Accounting for these geometrical changes in the solute would be important in the calculations of absorption spectra and other properties such as hyperpolarizability,[23] two-photon absorption cross section,[24] etc. We have shown that these geometrical changes in solute themselves account for 50% solvatochromic shift, in the case of nile red.[25] Moreover, it has been shown that, in the case of phenol blue, molecular structures with different BLA values result in quite different hyperpolarizability (difference is of four times in magnitude).[23] There are other interesting studies which report relationships between first and second hyperpolarizabilities with BLA for a number of molecules.[18,26]

In this article, we have investigated the structure and absorption spectra of MOQB in water solvent and its solvatochromic shift when compared to a gas-phase or nonpolar environment. Due to the aforementioned reasons, modeling solvatochromism requires techniques that account for the solvent-induced and thermally induced geometrical changes in the solute. Moreover, since water is a polar solvent and is known to have site-specific interaction with solute molecule, it must be important to use a discrete solvent model for water during the property, i.e., absorption spectra calculation. So, we have adopted Car−Parrinello molecular dynamics (CPMD) within a hybrid quantum mechanics-molecular mechanics (QM/MM) framework[15,16] for studying the finite temperature structure of MOQB in water solvent. For obtaining finite temperature structure of MOQB in the gas phase, we have used CPMD[27] technique. The absorption spectra calculations for MOQB in water were carried out using time-dependent density functional theory with Coulomb attenuated B3LYP (CAMB3LYP) functional including the solvent molecules through continuum or semicontinuum approaches. For comparison, gas-phase spectra were also calculated using the same level of theory.

2. COMPUTATIONAL DETAILS

The hybrid QM/MM calculations require equilibrated solute−solvent structure as initial configuration which we have generated using molecular dynamics (MD) calculations. In the MD run, we have used HF/6-31+G(d,p)-optimized molecular structure (using Gaussian 09 software[28]) and GAFF force field[29] for MOQB. For water solvent, we have used the TIP3P force field.[30] The simulation was carried out in an orthorhombic box containing a single MOQB molecule and 9613 solvent molecules. The simulation box size was approximately, 68.1, 67.4, and 63.6 Å. The MD simulation was carried out in an isothermal−isobaric ensemble using Amber 8 software.[31] The time scale for the MD run was around 100 ps. The final equilibrated solute−solvent structure has been used as the initial configuration for the CPMD-QM/MM calculation. Here, the MOQB is treated at density functional theory level while the solvents are treated using TIP3P force field. The QM/MM implementation includes the interaction between the QM and MM systems which involves electrostatic, short-range repulsion, and long-range dispersion interactions. This takes into account the polarization of the QM region due to the instantaneous electric field generated by the atomic charges of MM atoms. In our present calculations, for the description of QM region we have used the Becke, Lee, Yang, and Parr (BLYP) gradient-corrected functional[32,33] and the Troullier−Martins norm conserving pseudopotentials.[34] Here, the electronic wave function is expanded in a plane wave basis set. The energy cutoff of 80 Ry has been used. We have used 5 au as the time step for the integration of the equation of motion and 600 amu as the fictitious electronic mass. The CPMD calculations involve subsequent scaling and Nose runs where the former one brings the system temperature to 300 K. In the Nose run, the solute−solvent system samples canonical ensemble. The total time scale for the production run is 39 ps in the case of the MOQB−water system. In order to calculate the absorption spectra in nonpolar solvents, we have investigated the finite temperature structure of MOQB in the gas phase using CPMD simulation[27] with subsequent property calculations for the configurations in the trajectory. The total time scale for CPMD simulation of MOQB in the gas phase is 2 ps.

The absorption spectra for MOQB in water were computed for 50 configurations picked at equal intervals from the total 30 ps CPMD-QM/MM trajectory. The absorption spectra calculations were carried out at CAMB3LYP[35,36] level of theory using 6-31+G-(d,p) basis set. For the trajectory of MOQB in water, three sets of absorption spectra calculations were carried out using Gaussian 09[28] software. (i) The first set of calculations were carried out only for MOQB molecule alone (without solvents included) and this set of calculations will be referred to as MM0. (ii) Another set of calculations were carried out for MOQB molecule and by treating the solvents using conductor-like polarizable continuum model.[37] These results will be referred to as MM1. (iii) The third set of calculations were carried out for MOQB in water by treating

solvents using a semicontinuum approach[38] and the results will be referred to as MM2. In this approach, the solvent molecules involved in hydrogen bonding and charge transfer were treated using a discrete approach and are explicitly included in the QM region. All other remaining solvents were treated using conductor-like polarizable continuum model. For this purpose, we have computed solute-all-atoms and solvent center of mass ($g(r_{X-O})$) radial distribution function (rdf) (see Figure 1sa of the Supporting Information) which has been computed using the distances between the solute atoms and solvent center of mass. In this rdf, all the "influential" solvent molecules appear below a distance r = 2.9 Å. The shoulder appearing at this distance includes all the solvent molecules in the hydration shell. We have earlier reported[25,39] for the property calculations that the solvation shells based on $g(r_{X-O})$ rdf are highly desirable and convenient when compared to those obtained from usual center of mass rdf. The number of solvent molecules in the hydration shell of MOQB varies between 3 and 20, and the average number of solvent molecules is approximately 11 (see Figure 1sb of the Supporting Information). We have included all these "hydration shell" solvent molecules explicitly in the absorption spectra calculations. Figure 2s of the Supporting Information shows a snapshot of MOQB and solvent molecules in the first solvation shell. These three sets of calculations give insight into different contributions to the absorption spectra of MOQB in water. The MM0 results are obtained from the trajectory of MOQB in water and it includes only the contribution from solvent-induced geometrical changes since in the property calculation the solvents are not included explicitly or implicitly. The MM1 results include the contributions from solvent-induced geometrical changes and from solvent effect included using a continuum approach. So, this does not account for the contributions from hydrogen bonding and intermolecular charge transfer effect which have been accounted in the MM2 results. Overall, the MM2 calculations with a semicontinuum approach provide more accurate and realistic description of solvents since we define the influential solvent molecules using discrete approach (by explicitly including in the QM region) while the remaining solvents (which are not in immediate contact and direct interaction with solute) are treated using continuum approach which is sufficiently good. Finally, another set of calculations were carried out for 50 configurations obtained from the CPMD trajectory corresponding to MOQB in the gas phase. The calculated absorption spectra can be compared to the experimental spectra obtained for MOQB in nonpolar solvents. Moreover, the solvatochromic shift in the absorption spectra can be obtained from the shift in spectra calculated for the gas phase of MOQB and in water solvent.

3. RESULTS AND DISCUSSION

3.1. Solvent Dependence of Structure of MOQB. Usually, the solvatochromic molecules show larger changes in molecular geometry as a function of solvent polarity which can be seen from the average BLA values. The BLA has been recognized as an important structural quantity which has been directly related to nonlinear optical response of a molecule. There have been numerous studies in the literature on tuning BLA using electric field or solvents of varying polarity to extract the structure−property relationship.[26] The MOQB being a solvatochromic molecule, it is rewarding to investigate its molecular geometry in the gas phase and in water solvent. Due to the bridging of the phenyl rings, it is difficult to define the BLA but rather one can look into the bond lengths of C−O and C−NH_3 groups of MOQB. In the neutral

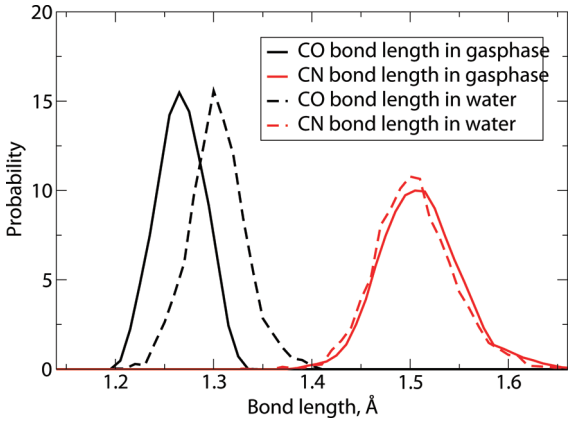

Figure 2. CO and NC bond lengths distribution of MOQB in the gas phase and in water solvent.

form, the CO bond length should have double bond character while in the charge-separated zwitterionic form the CO bond length should have a σ bond character. Since it has been proposed that the MOQB is in neutral form in the gas phase while in water it is in a charge-separated form,[9] one should expect increase in CO bond length due to increase in σ character when going from gas phase to water solvent. From Figure 2, which shows the CO and CN bond length distributions in the gas phase and in water, the average CO bond lengths in the gas phase and in water solvent are respectively 1.27 and 1.31 Å. The usual C═O and C−O bond lengths are respectively 1.23 and 1.43 Å. In water solvent, even though the C−O bond length is increased, it is not substantial when compared to standard double and single CO bond lengths which can be even attributed to bond stretching due to hydrogen bonding with water solvent. However, this appears to be larger when compared to water solvent-induced CO bond length increase in acetone reported based on similar CPMD-QM/MM calculations.[40] The increase in C−O bond length for acetone in water solvent is 0.02 Å while in the present case it is 0.04 Å. We have reported in the case of phenol blue that, with change in solvent from chloroform to water, the CO bond length increased similar to the present study.[17] Similarly, the solvent effect on C═O bond length and the subsequent blue shift in the absorption spectra have been reported in the literature by others.[40−42] Even though there is significant change in the CO bond length of MOQB, the CN bond length remains the same (1.51 Å) both in the gas phase and in water.

In the charge-separated form of a solvatochromic molecule, the charges are accumulated on the donor and acceptor groups which eventually leads to a larger dipole moment for the molecule in this state. In the case of *o*-betaine from similar CPMD-QM/MM calculations, we have reported that the group charges associated with pyridinium and phenoxide rings are respectively 0.73 and −0.73 q/e in water solvent and in the gas phase these are respectively 0.53 and −0.53 q/e.[22] Recently, we have reported a similar observation in the case of stilbazolium merocyanine in water.[43] These two molecules remain in charge-separated form in water. In the case of MOQB, due to the bridging of aromatic phenyl rings, we have computed the donor (D), acceptor (A), and bridge (B) group charges in the gas phase and in water solvent separately. The D-group charge is calculated by summing the average charges of atoms 1, 4, 5, 6, 7, 13, 14, and 15 (for numbering refer to Figure 1). The B-group charge is calculated from atomic charges of atoms 3 and 8 while the A-group charge is calculated from charges of atoms 2,

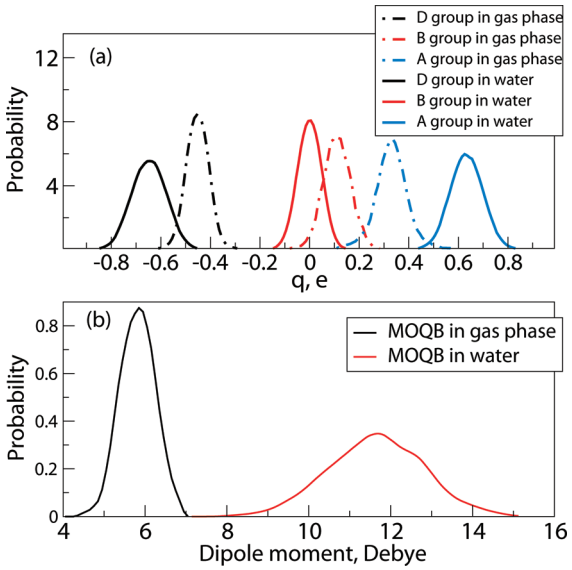

Figure 3. (a) Group charge distribution of MOQB in the gas phase and in water. (b) Dipole moment distribution of MOQB in the gas phase and in water.

9, 10, 11, 12, 16, 17, 18, 19, 20, and 21. The charges of MOQB in water are D-RESP[44] type charges and in the case of gas phase we have used ESP charges. These charges are obtained by fitting procedure to reproduce molecular electrostatic potential at number of points in a grid around the molecule. The D-resp charges refer to dynamically generated restrained electrostatic potential charges. The D-resp charges obtained from CPMD QM/MM calculations are dynamical quantities which evolve in time and depend on chemical state of solute and instantaneous solvent environment. The group charge distributions for MOQB in the gas phase and in water are shown in Figure 3a. The average D, B, and A group charges of MOQB in the gas phase are respectively −0.44, 0.11, and 0.33 q/e while in water solvent the group charges are respectively −0.64, 0.00, and 0.64. This shows that the MOQB molecule is polarized by water solvent significantly when compared to gas phase. We have also looked into the molecular dipole moment. We have calculated the dipole moment distribution for MOQB in the gas phase and in water solvent which is shown in Figure 3b. The molecular dipole moment is the first moment of charge distribution which has been computed using the formula

$$\overline{\mu} = \sum_{i=1}^{n} q_i \overline{r}_i \qquad (1)$$

where the q_i and $\overline{r}_i$ are the charges and position vector for the ith atom, respectively, and n is the number of atoms in MOQB molecule. Figure 3b shows the dipole moment distribution of MOQB in the gas phase and in water solvent. The average dipole moments in the gas phase and in water solvent are respectively 6 and 12 D. The dipole moment in water is almost 2 times larger than its gas-phase value. Both the group charge distribution and dipole moment distribution of MOQB in the gas phase and in water suggest that the MOQB is closer to a charge-separated form in water solvent. Moreover, a larger width in the dipole moment distribution for MOQB in water is seen which has to be attributed to solvents anisotropy.

3.2. Absorption Spectra and Solvatochromic Shift of MOQB. In this section, we discuss the absorption spectra of

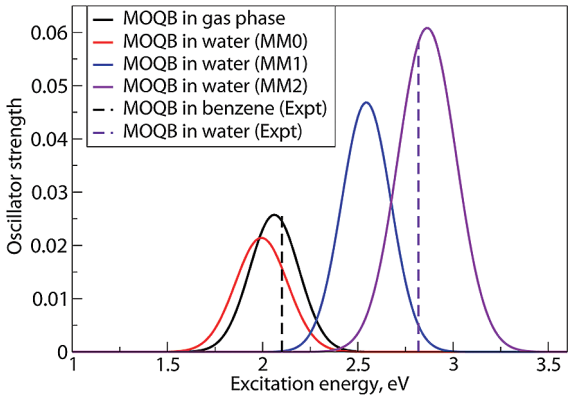

Figure 4. Distribution of $\pi-\pi^*$ excitation energy for MOQB in the gas phase and in water.

MOQB in the gas phase and in water and the solvatochromic shift and different contributions to the absorption spectra in water. Particularly, we are only interested in the low-energy excitation responsible for solvatochromic shift. In the negative solvatochromic molecules, this excitation usually has been attributed to $\pi-\pi^*$ type.[10] The absorption spectra of MOQB in polar and nonpolar solvents display two bands; one appearing beyond 400 nm and the one appearing below 400 nm.[4] The first band has been reported to be strongly dependent on the dielectric media, and the transition energy associated with this band can be used as polarity parameter (referred as E_{QB}), similar to Kosower's Z and Dimroth et al.'s $E_T(30)$ values.[45,46] Kosower's Z value and $E_T(30)$ were obtained from spectral behavior of 1-ethyl-4-carbomethoxy pyridinium (ECMP) and Reichardt's dye, respectively. Linear relationships have been reported between Z and $E_T(30)$ with E_{QB}, suggesting that MOQB is good polarity indicator as the ECMP and Reichardt's dye[4] (see eqs 2 and 3).

$$Z = 2.52E_{QB} - 68.4 \qquad (2)$$

$$E_T(30) = 1.712E_{QB} - 49.1 \qquad (3)$$

In the case of MOQB, the band corresponding to the lowest energy excitation is due to the transition from dipolar ground state to neutral excited state. The HOMO and LUMO molecular orbitals involved in the excitation are shown in Figure 3s of the Supporting Information. As can be seen, in HOMO the electron density is localized on the oxygen atom and aromatic ring connected to oxygen atom while in LUMO, the electron density is localized on N-methyl group and aromatic ring connected to this group. With increasing polarity of the solvent, the ground state becomes more stable which eventually leads to increase in excitation energy and subsequent blue shift in the spectra. This band appears around 590 nm in the case of benzene which blue shifts to 485 nm in absolute alcohol and it further blue shifts to around 440 nm in water solvent.[4,11] We have looked into this solvatochromic band. Figure 4 displays the distribution of excitation energy for the first excitation. The excitation energy distribution curve has been evaluated using the following formula:[47]

$$f(E) = \langle f \rangle \exp\left(-\frac{(E-\langle E \rangle)^2}{2\sigma^2}\right) \qquad (4)$$

where $\langle f \rangle$ and $\langle E \rangle$ are the averaged oscillator strength and the averaged excitation energy for the lowest excitation, respectively. Here, σ is the standard deviation of the lowest excitation energy

dx.doi.org/10.1021/jp1049342 |J. Phys. Chem. B 2011, 115, 1056–1061

Table 1. Average Excitation Energy and Solvatochromic Shift

system	λ_{max}, nm
MOQB gas phase	602
MOQB in water (MM0)	622
MOQB in water (MM1)	487
MOQB in water (MM2)	433
MOQB in benzene (expt)[11]	590
MOQB in absolute alcohol (expt)[11]	485
MOQB in water (expt)[4]	440
solvatochromic shift	169

calculated for all configurations in the trajectory. Overall, the distribution curve shown here does not have any arbitrary parameter. Usually, a bandwidth around 0.19 eV is used for the Gaussian fitting of simulated absorption spectra.[48] But in the present case, the width of the curve is associated with the second moment of the excitation energies and is due to the thermal and solvents anisotropies in the solute−solvent system. Figure 4 shows the excitation energy distribution curve for MOQB in the gas phase and for MOQB in water solvent with different solvent descriptions, namely MM0, MM1, and MM2 as explained earlier in section 2. As the configurations have been generated from the Car−Parrinello molecular dynamics calculations, the excitation energy can be simply calculated as an average over the excitation energies for all configurations. The calculated average excitation energies are reported in Table 1. Since we are not aware of the excitation energy reported for MOQB in the gas phase, the calculated gas-phase spectra can be compared to the spectra reported in nonpolar solvents.[4,11] The reported λ_{max} value in benzene is around 590 nm with which the simulated gas-phase spectra (with λ_{max} 602 nm) agrees very well. The experimental absorption maximum for MOQB in water solvent is around 440 nm.[4,11] Our calculated absorption spectra with a semicontinuum approach (i.e., MM2 model) is 433 nm which is in excellent agreement with this value. As we increase the solvent description from none to semicontinuum model, there is improvement in the calculated spectra. The λ_{max} for MM0 model is 622 nm which lies very close to the spectra in benzene. Interestingly, the λ_{max} from MM0 model is red-shifted when compared to the gas-phase value and this has to be attributed to the solvent-induced geometrical changes in CO bond length. Particularly, it is quite interesting to observe that solvent-induced geometrical changes bring red shift similar to nile red and phenol blue which are, in contrast, positive solvatochromic molecules.[25,39] A similar red shift in spectra has been reported by Blair et al. for formaldehyde in water from the calculations on solute alone (similar to our MM0 model) while the experimentally reported blue shift was obtained when the solvent molecules were included explicitly (similar to our MM2 model) in the calculations.[41] Similar to that in the present case, that study reports red shift in absorption spectra from MM0 model which has been attributed to the increase in CO bond length.[41] The observed shift due to geometrical change in MOQB is smaller (i.e., 12%) of the total solvatochromic shift when compared to 50% solvatochromic shift as seen in nile red.[25] With the continuum description for solvents (i.e., MM1 model), the calculated solvatochromic shift gains correct sign, i.e., a blue shift similar to experimental results.[4,11] It is quite interesting to find that the continuum model for solvents could reproduce the blue shift correctly but the magnitude of λ_{max} is ≈75 nm less when compared to experimental

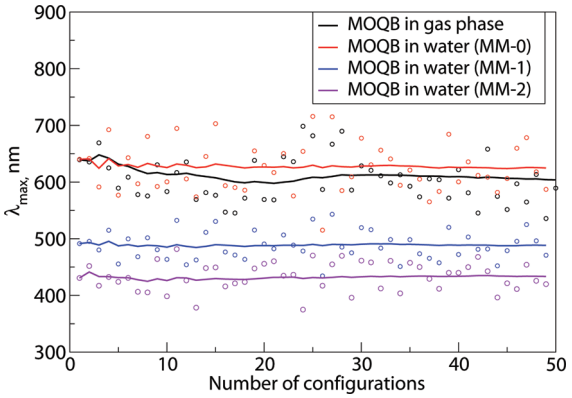

Figure 5. Instantaneous and *N*-point average of excitation energy for MOQB in the gas phase and in water (for all three models, namely MM0, MM1, and MM2).

value. This deviation is in line with previous reports on the absorption spectra of organic solute molecules in water solvent where the site-specific interactions and charge transfer have been proven to be important.[38,49] So, a discrete description for "influential" solvent molecules should bring further improvement in the calculated solvatochromic shift and absorption maximum and that is exactly what we see from the results corresponding to semicontinuum approach, i.e., MM2 model. Since the solvent molecules in the hydration shell are treated quantum mechanically, the hydrogen-bonding interaction and solute−solvent intermolecular charge transfer are accounted for explicitly. As mentioned earlier, the number of solvent molecules included explicitly is between 3 and 20 with an average number of solvent molecules equal to eleven in these calculations. The absorption maximum calculated using MM2 model is 433 nm which is in good agreement with experimental spectra (i.e., $\lambda_{max} \approx 440$ nm). By comparing MM1 and MM2 results, we come to a conclusion that hydrogen-bonding and site-specific solute−solvent interactions contributed 75 nm to the solvatochromic shift in the case of MOQB in water. The calculated solvatochromic shift from the MM2 model is approximately 170 nm. Overall, we find that the semicontinuum model can provide sufficiently accurate description for solvent molecules in the absorption spectra calculations and still it is computationally less demanding as only the "influential" solvent molecules are treated using a discrete approach. Finally, we have also tested for the convergence of absorption spectra (for both MOQB in the gas phase and in water solvent) with number of configurations. For this we have plotted instantaneous and *N*-point average of λ_{max} with increasing number of configurations. The results are shown in Figure 5 which clearly indicates the λ_{max} is converged with number of configurations in the gas phase and in MM0, MM1, and MM2 models of MOQB in water. Even though in the case of MM2 model the number of solvents varies between 3 and 20, we do not see any increased width in the excitation energy distribution curve (Figure 4) when compared to MM1 and MM0 models. Moreover, the *N*-point average of λ_{max} is converged within 20 configurations for this model similar to other models.

3.3. Conclusions. In the current work we have used a combined CPMD-QM/MM and semicontinuum approach to calculate finite temperature structure and the electronic excitation energy of the MOQB in water, respectively. We have shown that this combined approach is capable of reproducing accurately the absorption spectra of MOQB in water. We have also calculated spectra for the gas phase which is again in good agreement with

spectra in benzene, a nonpolar solvent, and overall the calculations reproduce the solvatochromic shift in good agreement. We have found that the solvent-induced geometrical changes result in red shift in the absorption spectra as reported earlier in the case of formaldehyde.[41] A continuum model for solvents could reproduce the correct order for solvatochromic shift but quantitatively underestimates the λ_{max} by ≈75 nm. Finally, a semicontinuum approach excellently reproduces the experimental absorption spectra of MOQB in water. The semicontinuum approach includes all important contributions such as intermolecular charge transfer and hydrogen-bonding effect due to hydration shell solvents, and uses continuum solvent description for the solvent molecules beyond hydration shell. Still, it is computationally less demanding as only the solvent molecules in the hydration shell are included. Overall, the current work supports the use of MOQB as polarity indicator for microcavity in proteins, reverse micelles, etc. It is shown to have comparatively larger solvatochromic shift similar to Reichardt's dye but due to its advantageously smaller size the former can be used for the characterization applications of the proteins with smaller binding cavities.

■ ASSOCIATED CONTENT

Supporting Information. Solute all-atoms and solvent center of mass ($g(r_{X-O})$) rdf and the time evolution of number of solvent molecules in the first solvation shell; snapshot of MOQB and its first solvation shell structure; and LUMO and HOMO molecular orbitals of MOQB in water. This material is available free of charge via the Internet at http://pubs.acs.org.

■ AUTHOR INFORMATION

Corresponding Author
*E-mail: murugan@theochem.kth.se.

■ ACKNOWLEDGMENT

This work was supported by a grant from the Swedish Infrastructure Committee (SNIC) for the project "Multiphysics Modeling of Molecular Materials", SNIC 023/07-18. The author gratefully acknowledges support and encouragement from Prof. Hans Ågren and the financial support received from MONAMI INDO-EU project.

■ REFERENCES

(1) Latypov, R. F.; Liu, D.; Gunasekaran, K.; Harvey, T. S.; Razinkov, V. I.; Raibekas, A. A. *Protein Sci.* **2008,** *7* (4), 652.
(2) Hawe, A.; Sutter, M.; Jiskoot, W. *Pharm. Res.* **2007,** *25*, 1487.
(3) Drummond, C. J.; Grieser, F.; Albers, S. *Colloids Surf.* **1991,** *54*, 197.
(4) Ueda, M.; Schelly, Z. A. *Langmuir* **1989,** *5*, 1005.
(5) Reichardt, C. *Pure Appl. Chem.* **2004,** *76* (10), 1903.
(6) Drummond, C. J.; Grieser, F.; Healy *J. Phys. Chem.* **1988,** *4*, 217.
(7) Healy, T. W.; Drummond, C. J.; Grieser, F.; Murray, B. S. *Langumir* **1990,** *6*, 506.
(8) Murray, B. S.; Drummond, C. J.; Grieser, F.; White, L. R. *J. Phys. Chem.* **1990,** *94*, 6804.
(9) Kumoi, S.; Oyama, K.; Yano, T.; Kobayashi, H.; Ueno, K. *Talanta* **1970,** *17*, 319.
(10) Reichardt, C. *Chem. Rev.* **1994,** *94*, 2319.
(11) Philips, J. P.; Keown, R. W. *J. Am. Chem. Soc.* **1951,** *73*, 5483.
(12) Canuto, S.; Coutinho, K.; Trzesniak, D. *Adv. Quantum Chem.* **2002,** *41*, 161.
(13) Aidas, K.; Kongsted, J.; Osted, A.; Mikkelsen, K. V.; Christiansen, O. *J. Phys. Chem. A* **2005,** *109*, 8001.
(14) Roitberg, A. E.; Worthington, S. E.; Holden, M. J.; Mayhew, M. P.; Krauss, M. *J. Am. Chem. Soc.* **2009,** *122*, 7312.
(15) Warshel, A.; Levit, M. *J. Mol. Biol.* **1976,** *103*, 227.
(16) Field, M. J.; Bash, P. A.; Karplus, M. *J. Comput. Chem.* **1990,** *11* (6), 700.
(17) Murugan, N. A.; Rinkevicius, Z.; Ågren, H. *J. Phys. Chem. A* **2009,** *113*, 4833.
(18) Murugan, N. A.; Rinkevicius, Z.; Kongsted, J.; Ågren, H. *Proc. Natl. Acad. Sci. U.S.A.* **2010,** *107* (38), 16453.
(19) Gao, J.; Alhambra, C. *J. Am. Chem. Soc.* **1997,** *119*, 296.
(20) Cammi, R.; Mennucci, B.; Tomasi, J. *J. Am. Chem. Soc.* **1998,** *120*, 8834.
(21) Fonseca, T. L.; Coutinho, K.; Canuto, S. *Chem. Phys.* **2008,** *349* (1−3), 109.
(22) Murugan, N. A.; Agren, H. *J. Phys. Chem. A* **2009,** *113*, 2572.
(23) Serrano, A.; Canuto, S. *Int. J. Quantum Chem.* **2002,** *87* (5), 275.
(24) Pati, S. K.; Marks, T. J.; Ratner, M. A. *J. Am. Chem. Soc.* **2001,** *123*, 7287.
(25) Murugan, N. A.; Rinkevicius, Z.; Ågren, H. *Int. J. Quantum Chem.* **2010,** *00*, 00.
(26) Marder, S. R.; Beratan, D. N.; Cheng, L. T. *Science* **1991,** *252*, 103.
(27) Hutter, J.; Parrinello, M.; Marx, D.; Focher, P.; Tuckerman, M.; Andreoni, W.; Curioni, A.; Fois, E.; Röthlisberger, U.; Giannozzi, P.; Deutsch, T.; Alavi, A.; Sebastiani, D.; Laio, A.; VandeVondele, J.; Seitsonen, A.; Billeter, S. Computer code CPMD, version 3.11, Copyright IBM Corp. and MPI-FKF Stuttgart, 1990−2002.
(28) Frisch, M. J.; et al. *Gaussian 09, Revision A.1*; Gaussian, Inc.: Wallingford, CT, 2009.
(29) Wang, J.; Wolf, R. M.; Caldwell, J. W.; Kollman, P. A.; Case, D. A. *J. Comput. Chem.* **2004,** *25* (9), 1157.
(30) Jorgensen, W. L.; Chandrasekhar, J.; Madura, J. D.; Impey, R. W.; Klein, M. L. *J. Chem. Phys.* **1983,** *79*, 926.
(31) Case, D. A.; et al. *AMBER 8*; University of California: San Francisco, 2004.
(32) Becke, A. D. *Phys. Rev. A* **1988,** *38*, 3098.
(33) Lee, C.; Yang, W.; Parr, R. C. *Phys. Rev. B* **1988,** *37*, 785.
(34) Trouiller, N.; Martins, J. L. *Phys. Rev. B* **1991,** *43*, 1993.
(35) Yanai, T.; Tew, D. P.; Handy, N. C. *Chem. Phys. Lett.* **2004,** *393*, 51.
(36) Peach, M. J. G.; Helgaker, T.; Salek, P.; Keal, T. W.; Lutns, O. B.; Tozer, D. J.; Handy, N. C. *Phys. Chem. Chem. Phys.* **2006,** *5*, 558.
(37) Klamt, A. *J. Phys. Chem.* **1995,** *99*, 2224.
(38) Besley, N. A.; Hirst, J. D. *J. Am. Chem. Soc.* **1999,** *121*, 8559.
(39) Murugan, N. A.; Jha, P. C.; Rinkevicius, Z.; Ruud, K.; Ågren, H. *J. Chem. Phys.* **2010,** *123*, 234508.
(40) Röhrig, U. F.; Frank, I.; Hutter, J.; Laio, A.; VandeVondele, J.; Rothlisberger, U. *Chem. Phys. Chem.* **2003,** *4*, 1177.
(41) Blair, J. T.; Jespersen, K.K-.; Levy, R. M. *J. Am. Chem. Soc.* **1989,** *111*, 6948.
(42) Dilling, W. L. *J. Org. Chem.* **1966,** *31*, 1045.
(43) Murugan, N. A.; Kongsted, J.; Rinkevicius, Z.; Aidas, K.; Ågren, H. *J. Phys. Chem. B* **2010,** *114*, 13349.
(44) Laio, A.; VandeVondele, J.; Röthlisberger, U. *J. Phys. Chem. B* **2002,** *106*, 7300.
(45) Kosower, E. M. *J. Am. Chem. Soc.* **1958,** *80*, 3253.
(46) Dimroth, K.; Reichardt, C.; Siepmann, T.; Bohlmann, F. *Ann. Chem.* **1963,** *661*, 1.
(47) Julia de Almeida, K.; Murugan, N. A.; Rinkevicius, Z.; Hugosson, H. W.; Vahtras, O.; Ågren, H.; Cesar, A. *Phys. Chem. Chem. Phys.* **2009,** *11*, 508.
(48) Choe, Y. K.; Negase, S.; Nishimoto, K. *J. Comput. Chem.* **2007,** *28*, 727.
(49) Han, W.-G.; Liu, T.; Himo, F.; Toutchkine, A.; Bashford, D.; Hahn, K. M.; Noodleman, L. *Chem. Phys. Chem.* **2003,** *4*, 1084.